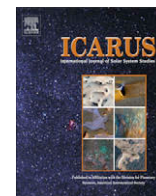




Contents lists available at ScienceDirect

Icarus

journal homepage: www.elsevier.com/locate/icarus

Note

Radar observations of 8P/Tuttle: A contact-binary comet

John K. Harmon^{a,*}, Michael C. Nolan^a, Jon D. Giorgini^{b,1}, Ellen S. Howell^a^a National Astronomy and Ionosphere Center, Arecibo Observatory, HC3 Box 53995, Arecibo, PR 00612, USA^b Jet Propulsion Laboratory, California Institute of Technology, MS 301-150, 4800 Oak Grove Dr., Pasadena, CA 91109, USA

ARTICLE INFO

Article history:

Received 30 September 2009

Revised 16 December 2009

Accepted 17 December 2009

Available online xxxxx

Keywords:

Comets

Comets, Nucleus

Radar observations

ABSTRACT

Arecibo radar imagery of Comet 8P/Tuttle reveals a 10-km-long nucleus with a highly bifurcated shape consistent with a contact binary. A separate echo component was also detected from large (>cm-size), slow-moving grains of the type expected to contribute to the Ursid meteor stream.

© 2009 Elsevier Inc. All rights reserved.

1. Introduction

8P/Tuttle is a high-inclination, Halley-type comet in a 13.5-year orbit. Although Tuttle had been observed at a dozen apparitions since its 1858 discovery, little was known about the nucleus itself. A single nucleus radius estimate of 7.3 km, based on telescopic photometry and an assumed visual albedo of 4% (Licandro et al., 2000), suggested that Tuttle is a relatively large comet in the Halley size class. Tuttle had also been identified as the parent of the Ursid meteor stream (Jenniskens et al., 2002), which implies that the nucleus sheds debris.

Tuttle's relatively close ($\Delta = 0.25$ AU) Earth passage on January 2, 2008 placed the comet favorably for Arecibo radar observations. It was anticipated that delay-Doppler radar imaging should yield at least a direct nucleus size estimate (Harmon et al., 2004), although the distance would be too great for imaging detailed surface structure. We observed the comet with the Arecibo radar on four consecutive days immediately following close approach. These observations produced a sequence of delay-Doppler images from which we deduced the size, shape and rotation of the nucleus. This is only the third comet to be imaged by radar, after P/2005 JQ5 (Catalina) (Harmon et al., 2006) and the split comet 73P/Schwassmann-Wachmann 3 (Nolan et al., 2006b). The new Tuttle imagery is especially interesting as it has revealed a strongly bifurcated nucleus consistent with a contact binary. We also identified a separate echo component from large grains in the inner coma, which confirms Tuttle as a source of slow-moving debris. In this paper we present our radar results for Comet Tuttle and discuss the potential implications for binary comets.

2. Observations

The observations were made with the Arecibo S-band (2380 MHz; $\lambda = 12.6$ cm) radar on the four consecutive dates January 2–5, 2008. We transmitted a 630 kW, circularly polarized wave and received the echo in both (orthogonal) circular polarizations; these two polarization senses are here denoted “OC” (for Opposite Circu-

lar), the expected sense for specular reflection, and “SC” (for Same Circular), which is a weaker component associated with depolarization by small-scale roughness (Ostro, 1993). We employed two different observing modes based on different transmission schemes. The first mode consisted of range-resolved observations designed for radar imaging the nucleus by the delay-Doppler method (Ostro, 1993); in this mode we did a binary-phase-coded transmission with a 2- μ s “baud” (synthesized pulse width), which gave a 300-m range resolution for the images. In the second mode we did an unmodulated or continuous-wave (CW) transmission designed to measure the total Doppler spectrum only; this is the better method for measuring radar cross sections and polarization ratios and for identifying any broadband echo component from large ejected grains. Each day's observing session consisted of from 12 to 18 transmit/receive cycles (“runs”), with each run being two light-travel round-trips (~8.7 min) in length. A mix of CW and delay-Doppler observations was done on each of the first three dates, whereas the last date was devoted solely to delay-Doppler imaging.

3. Nucleus

Usable delay-Doppler images (Fig. 1) of the nucleus were obtained in the OC polarization on all four observing dates. Each image in Fig. 1 is the sum of three successive runs and spans 21 min. The minimum time lapse between successive images was 26 min and the total time span covered by imaging on a given day (limited by the Arecibo telescope's 2.7-h tracking window) varied between 55 min (January 2) and 2.6 h (January 3). The nucleus rotation and bilobate shape are both apparent from these images. An inter-day comparison of the images shows that the same rotation phase repeats after about 23 h. This one-day rotation aliasing, combined with Arecibo's short daily observing window, had the unfortunate effect of limiting our overall rotation phase coverage and allowing us a good view of only one side of the nucleus. Nevertheless, with this caveat, we can definitely say that the radar images are consistent with a contact binary. We base this on the fact that the cleft between the two lobes (when the nucleus is observed broadside) is as deep as the delay depth at the two limbs, implying a connecting neck that has little or no width.

To quantify various nucleus characteristics we fit the delay-Doppler images in Fig. 1 with an idealized shape model based on a contact binary composed of prolate spheroidal lobes aligned along the binary axis. The model also assumed the nucleus to be in principal-axis (PA) rotation with a spin vector perpendicular to the long

* Corresponding author. Fax: +1 787 878 1861.

E-mail addresses: harmon@naic.edu (J.K. Harmon), nolan@naic.edu (M.C. Nolan), jon.d.giorgini@jpl.nasa.gov (J.D. Giorgini), ehowell@naic.edu (E.S. Howell).¹ Fax: +1 818 393 6388.

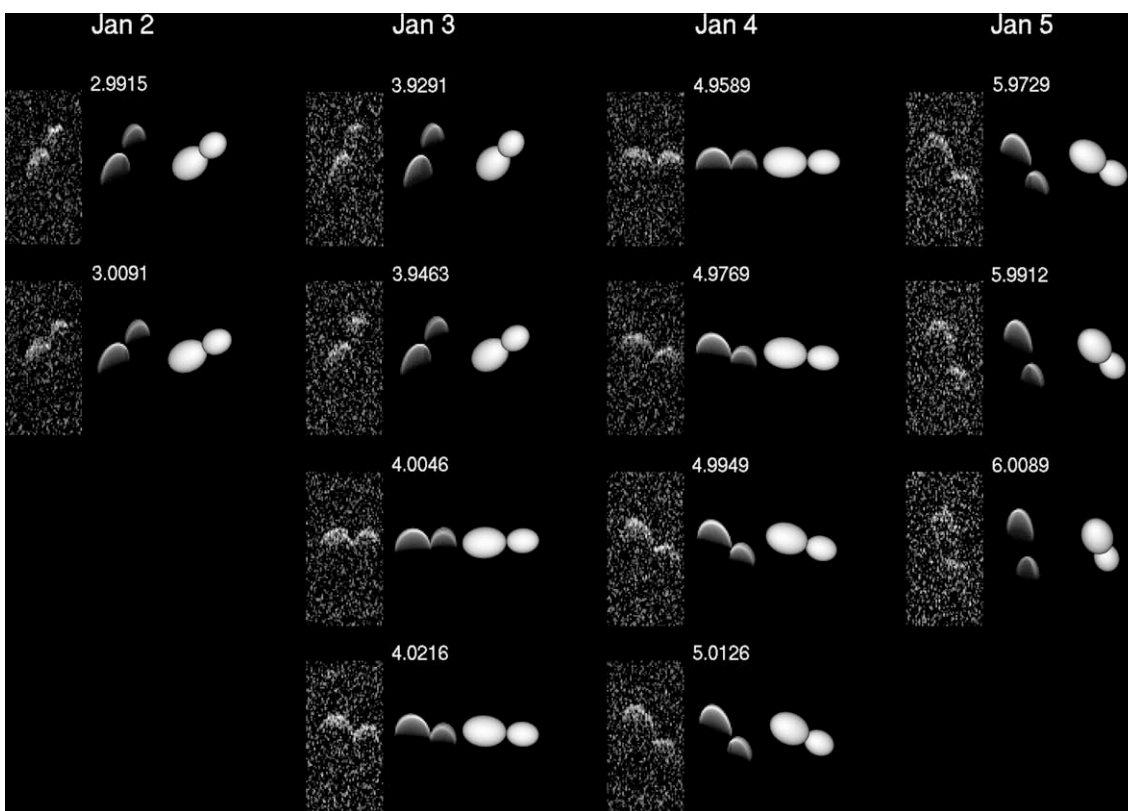


Fig. 1. Radar images (OC polarization) of the Comet Tuttle nucleus and corresponding best-fit model. The images for each date are arranged vertically, with the date atop that column corresponding to the UT date at the start of the observing session. At each epoch we show the delay-Doppler radar image (left), the model delay-Doppler array (middle), and the model figure in plane-of-sky projection (right). Each image is the sum over a 21-min time span centered on the indicated mean UT epoch (January decimal day number). Each delay-Doppler image rectangle measures $100 \mu\text{s}$ (15 km) in delay (vertical axis) by 25 Hz (1.58 m s^{-1}) in Doppler (horizontal axis). The pixel resolution is $1 \mu\text{s} \times 0.5 \text{ Hz}$.

(binary) axis. We performed an iterative nonlinear least squares fit of the model to the entire ensemble of 13 images, varying eight free parameters (three rotation parameters, four shape parameters, and a scattering parameter). The rotation parameters were the synodic rotation period P , the rotation phase φ , and the sub-Earth latitude δ (the complement of the angle between the spin axis and the line of sight). The shape parameters were a projected length parameter $L_c \equiv L \cos \delta$ (where L is the total long-axis length), the ratio of the lobe lengths, and the axial ratios of the two lobes. The scattering parameter was the exponent n in the assumed $\sigma^\circ(i) \propto \cos^n i$ scattering law, where $\sigma^\circ(i)$ is the “specific radar cross section” (per unit surface area) and i is the incidence angle between the line of sight and the surface normal.

The best-fit model is shown in Fig. 1. Here, for each of the 13 image epochs, we show the model delay-Doppler array as well as the model figure in plane-of-sky projection. Our most accurately determined parameter is the synodic rotation period, for which we estimate $P = 11.385 \pm 0.004 \text{ h}$. The rotation phase at the reference epoch of January 4.0046 (the mean time of the third image on day 2) was $\varphi = -5 \pm 1.5^\circ$, where we define zero phase as when the nucleus is observed broadside with the larger lobe approaching. Our modeling was only moderately sensitive to the sub-Earth latitude δ , although we were able to derive a crude estimate of $\delta = 35 \pm 7^\circ$. Aside from δ , our modeling could not constrain the spin-axis direction owing to insufficient pole aspect change over the four-day radar campaign. This also prevented us from determining the true (sidereal) rotation period, although the comet’s $4^\circ/\text{day}$ sky motion indicates that it must be within 0.06 h of the synodic period. To test the hypothesis of PA rotation, we allowed the fitting algorithm to vary the angle θ between the spin axis and the binary axis. The fits showed θ to be within a half-degree of 90° , providing strong support for a PA (or unexcited) rotation state. For our projected length parameter we estimate $L_c = 8.22 \pm 0.12 \text{ km}$, from which we derive a total long-axis dimension $L = 10.0 \pm 0.9 \text{ km}$ (the error mainly reflecting the large uncertainty in δ). The lobes have measurably different sizes, with one longer by a factor of 1.35 ± 0.04 . We find that the larger lobe is well characterized by a spheroid of axial ratio 1.4, whereas the smaller lobe is slightly less elongated (axial ratio 1.3) and more irregular (showing facets). These numbers translate to spheroidal dimensions of $5.75 \times 4.11 \text{ km}$ and $4.25 \times 3.27 \text{ km}$ for the larger and smaller lobes, respectively, and a lobe mass ratio of 2.14 (assuming equal densities). The combined lobe dimensions correspond to a broadside projected area of 30 km^2 or an effective radius of 3.1 km. We find, then, that the Tuttle nucleus is significantly smaller than the $\sim 7 \text{ km}$ radius deduced by Licandro et al. (2000), and more recently

by Snodgrass et al. (2008) and Weissman et al. (2008), from CCD photometry at large heliocentric distance (where the coma contribution is expected to be small). Since these photometric estimates all assumed a visual albedo of 4%, one way to reconcile with the smaller radar-derived size would be to invoke a much higher visual albedo of 20%. However, this conflicts with recent Hubble Space Telescope (HST) observations (Lamy et al., 2008), which deduced a size similar to our radar estimate when assuming the canonical 4% albedo. Furthermore, the smaller nucleus size is supported by thermal measurements with the Spitzer Space Telescope (Groussin et al., 2008) and the Plateau de Bure interferometer (Boissier et al., 2009) at infrared and mm wavelengths, respectively. The HST light curves (Lamy et al., 2008) also support our 11.4-h rotation period. Observations of spiral coma jets (Woodney et al., 2008; Waniak et al., 2009) have also been used to argue for a 5.7-h period, in part because this would favor a simple single-jet model over one requiring two antipodal jets. However, we hold our 11.4-h period to be incontrovertible, which implies that the two-jet coma model must be taken seriously.

The radar observations also provide information on the surface characteristics of the Tuttle nucleus. Some of this can be gleaned from Fig. 2, which shows the CW Doppler spectra of the nucleus when oriented approximately broadside. The total (OC + SC) radar cross section obtained by integrating these spectra is 4.5 km^2 . Dividing this by the nucleus projected area (30 km^2) from our model gives a radar albedo of 0.15, which is considerably higher than the low (~ 0.05) values typical of other radar-detected comets (Harmon et al., 2004; Harmon and Nolan, 2005). Since the radar albedo is mainly sensitive to the bulk density of the top few meters, this implies that the Tuttle nucleus surface is relatively well compacted with a density in the range $0.9\text{--}1.8 \text{ g cm}^{-3}$ (where the low-density end of this range corresponds to an icy composition and the high end to a dusty composition; see Harmon et al., 2004). The radar scattering properties of the nucleus also provide information on surface roughness. The delay-Doppler model fit gave $n \approx 0.6$ for the scattering-law exponent. This, and the sharpness of the edges of the OC Doppler spectrum (Fig. 2), indicates that the nucleus is limb-brightened ($n < 1$), a condition diagnostic of considerable blocky roughness at super-wavelength scales (Evans, 1969; Harmon et al., 2004). Note that the OC spectrum in Fig. 2 has a bimodal shape reflecting the bilobate structure of the nucleus, whereas the SC spectrum is unimodal. This difference, which corresponds to high SC/OC polarization ratios in the cleft between the two lobes, implies a high concentration of multiply-scattering blocky debris in this region. Note also that the SC curve is skewed toward positive Dopplers, which indicates that the larger lobe is the rougher of the two lobes.

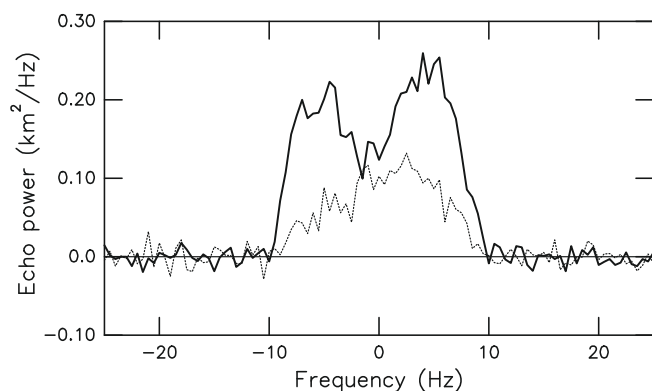


Fig. 2. Radar Doppler spectrum of the Tuttle nucleus from summation of the CW spectra from January 3 to 4, 2008. Shown are both circular polarization components: OC (solid line) and SC (dotted line). The mean rotation phase is -24.1° (where 0° is broadside) and the total phase span is 31° . The Doppler axis has been adjusted so that zero frequency is midway between the spectrum edges; on this scale the center-of-mass Doppler is estimated to be ≈ 0.9 Hz, based on equivalent Doppler spectra computed from our model.

4. Large-grain coma

In addition to the nucleus echo, the CW Doppler spectrum showed a broader echo component associated with backscatter off large (>cm-size) grains in the inner coma. This “grain-coma” echo (with nucleus subtracted) is shown in Fig. 3. The radar cross section of this component is 4.9 km^2 , or about the same as the nucleus echo. The 60-Hz bandwidth (FWHM) of the spectrum corresponds to a characteristic velocity dispersion of 4 m s^{-1} for the grains. Although the SC echo is relatively weak, the measured SC/OC circular polarization ratio $\mu_c = 0.14$ is sufficiently large to require the largest grains in the distribution to have radii larger than the Rayleigh–Mie transition size of $\lambda/2\pi$, or 2 cm (see Harmon et al., 1989, 2004; Nolan et al., 2006a). Such large, slow-moving grains are precisely the type expected to populate the Ursid meteor stream known to be associated with this comet (Jenniskens et al., 2002). The “peak-and-wings” shape of the spectrum is similar to that seen for other comets, as is the skew or asymmetry about zero Doppler (Harmon et al., 2004). The spectral shape and asymmetry are consistent with the preponderance of grains being ejected into escape trajectories rather than circumnuclear orbits (Harmon et al., 2004). The negative skew implies anisotropic grain ejection with a preference for ejection in directions away from the Earth. Since the Sun–comet–Earth angle was about 60° , this means that the grain ejection fan cannot have been strongly Sun-centered. The 4 m s^{-1} grain velocity dispersion falls toward the low end of the $1.4\text{--}21 \text{ m s}^{-1}$ range measured for radar grain comae, being closest to that measured for Comets C/IRAS-Araki-Alcock and 1P/Halley (Harmon et al., 2004). Escape trajectories with this velocity are physically plausible, since a simple gas-drag model (see Harmon et al., 2004) for this comet, assuming the nominal sublimation gas mass flux of $5 \times 10^{-5} \text{ g cm}^{-2}$, gives a terminal velocity of 6 m s^{-1} for 2-cm-radius grains and a maximum liftable grain radius of 4 cm. Finally, we note that this is the ninth of the 13 radar-detected comets to show a grain-coma echo, which

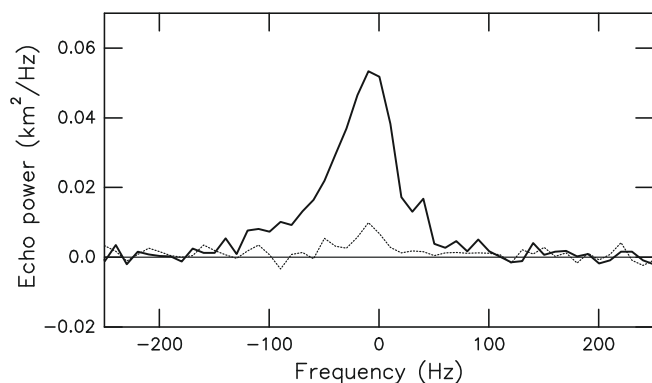


Fig. 3. Doppler spectrum of the echo from large ejected grains in the inner coma, summed over all CW spectra from January 2 to 4, 2008. The nucleus has been subtracted from this spectrum by interpolation. Shown are both circular polarization components: OC (solid line) and SC (dotted line). Note that the Doppler (horizontal) scale has been made a factor of 10 wider than for the nucleus (Fig. 2), in order to accommodate the much broader coma echo.

further underscores the importance and prevalence of large-grain ejection by comets (Harmon et al., 2004; Nolan et al., 2006a).

5. Binary comets

The most important finding from our Tuttle observations is the identification of an apparent contact-binary comet. Recent years have seen a proliferation of discoveries of binary objects among various minor-planet populations, including the near-Earth asteroids (NEAs), main-belt asteroids, Jupiter Trojans, Centaurs, and Kuiper Belt Objects (KBOs). Contact binaries alone are estimated to constitute 10–20% of all NEAs, Trojans, and KBOs (Sheppard and Jewitt, 2004; Noll et al., 2008; Mann et al., 2007; Benner et al., 2006, 2008). Since comets may be subject to some of the same dynamical processes and/or derive from the same primordial disk population as these other bodies, it has been argued that binary comets should exist and may even be common (Noll, 2006; Noll et al., 2006). Testing this hypothesis has been difficult, however, owing to the sparseness of the sample of comet nuclei that have been studied in detail. Prior to 2008 only six comet nuclei had been imaged by spacecraft or radar. Spacecraft images of Comet 19P/Borrelly revealed a peanut-shaped nucleus that has been suggested as a possible contact binary (Oberst et al., 2004). Comet 1P/Halley is also sometimes described as peanut-shaped and certainly shows some bilobate structure (Keller et al., 2004). Although neither of these comets could be considered to be strongly bifurcated, their complex elongate shapes raised the suggestion that some comet nuclei may be composed of coalesced fragments. Tuttle appears to be more strongly bifurcated than either Borrelly or Halley and offers the best evidence yet for the existence of contact-binary comets.

Binary and contact-binary minor planets are thought to form from collisions, mutual capture, or fission (Noll, 2006; Richardson and Walsh, 2006). Tuttle could have spun up to rotational fission through the action of outgassing torques, a close encounter with Earth (a possibility given the comet’s 0.997 AU perihelion), or a primordial close encounter with a large body in the protoplanetary disk. If the nucleus possesses some internal strength, rotational fission (a preferred process for binary NEAs) can produce a contact binary with a prolate primary like Tuttle’s (Walsh et al., 2008). Furthermore, a Tuttle-like alignment of the elongated fission products along the binary axis is known to be a stable, minimum-energy configuration (Scheeres, 2007). According to Scheeres’s model, Tuttle’s smaller or secondary lobe would be sufficiently massive (containing 32% of the total mass) to maintain the lobes gravitationally bound and in contact. It seems likely that the same alignment and stability conditions should hold even if the binary is not formed by spinup fission. Comet splitting appears to be a fairly common process that can be induced by other factors such as thermal or tidal stress. In fact, the propensity of comets for splitting has led to the suggestion that some splittings may result from the breakup of pre-existing contact binaries or other forms of cometary aggregates (Boehnhardt, 2004; Noll et al., 2006).

An alternative to fission is that Tuttle was formed by a mutual-capture process in the primordial Solar-System disk. Mutual capture, mediated by various proposed relaxation mechanisms, is the preferred method for constructing binary KBOs and Trojans (Weidenschilling, 2002; Goldreich et al., 2002; Astakhov et al., 2005; Mann et al., 2007). Some mutual-capture theories show a preference for forming close pairings of similar-size bodies, which could explain an object like Tuttle. Mutual-capture processes could have operated efficiently in the densely populated protoplanetary disk, after which any primordial binary pairs may have scattered adiabatically out to their current orbits under the action of giant-planet migration. Current theories have Jupiter-family comets coming from either the Kuiper belt or the Scattered Disk, long-period comets from the Oort Cloud, and Halley-type comets (like Tuttle) from the inner Oort Cloud or some other reservoir (Dones et al., 2004). If these various trans-neptunian comet reservoirs are the scattered remnants of the same protoplanetary disk population, then contact binaries may be as common in the comet population as in these other subpopulations and would not necessarily be peculiar to any particular comet family.

Acknowledgment

The National Astronomy and Ionosphere Center (Arecibo Observatory) is operated by Cornell University under a cooperative agreement with the National Science Foundation.

References

- Astakhov, S.A., Lee, E.A., Farrelly, D., 2005. Formation of Kuiper-belt binaries through multiple chaotic scattering encounters with low-mass intruders. *Mon. Not. R. Astron. Soc.* 360, 401–415.
- Benner, L.A.M., Nolan, M.C., Ostro, S.J., Giorgini, J.D., Pray, D.P., Harris, A.W., Magri, C., Margot, J.-L., 2006. Near-Earth Asteroid 2005 CR37: Radar images and photometry of a candidate contact binary. *Icarus* 182, 474–481.
- Benner, L.A.M., Nolan, M.C., Margot, J., Brozovic, M., Ostro, S.J., Shepard, M.K., Magri, C., Giorgini, J.D., Busch, M.W., 2008. Arecibo and Goldstone radar imaging of contact binary near-Earth asteroids. *Bull. Am. Astron. Soc.* 40, 432.
- Boehnhardt, H., 2004. Split comets. In: Festou, M.C., Keller, H.U., Weaver, H.A. (Eds.), *Comets II*. Univ. of Arizona Press, Tucson, pp. 301–316.

- Boissier, J., Bockelée-Morvan, D., Groussin, O., Biver, N., Colom, P., Crovisier, J., Jorda, L., Lamy, P., Moreno, R., 2009. The thermal emission of Comet 8P/Tuttle nucleus as observed with the Plateau de Bure interferometer. *Bull. Am. Astron. Soc.* 41, 1027.
- Dones, L., Weissman, P.R., Levison, H.F., Duncan, M.J., 2004. Oort Cloud formation and dynamics. In: Festou, M.C., Keller, H.U., Weaver, H.A. (Eds.), *Comets II*. Univ. of Arizona Press, Tucson, pp. 153–174.
- Evans, J.V., 1969. Radar studies of planetary surfaces. *Annu. Rev. Astron. Astrophys.* 7, 201–249.
- Goldreich, P., Lithwick, Y., Sari, R., 2002. Formation of Kuiper-belt binaries by dynamical friction and three-body encounters. *Nature* 420, 643–646.
- Groussin, O., Kelley, M., Lamy, P., Toth, I., Fernandez, Y., Jorda, L., Weaver, H., 2008. Spitzer Space Telescope observations of the nucleus of Comet 8P/Tuttle. *Bull. Am. Astron. Soc.* 40, 393–394.
- Harmon, J.K., Nolan, M.C., 2005. Radar observations of Comet 2P/Encke during the 2003 apparition. *Icarus* 176, 175–183.
- Harmon, J.K., Campbell, D.B., Hine, A.A., Shapiro, I.I., Marsden, B.G., 1989. Radar observations of Comet IRAS-Araki-Alcock 1983d. *Astrophys. J.* 338, 1071–1093.
- Harmon, J.K., Nolan, M.C., Ostro, S.J., Campbell, D.B., 2004. Radar studies of comet nuclei and grain comae. In: Festou, M.C., Keller, H.U., Weaver, H.A. (Eds.), *Comets II*. Univ. of Arizona Press, Tucson, pp. 265–279.
- Harmon, J.K., Nolan, M.C., Margot, J.-L., Campbell, D.B., Benner, L.A.M., Giorgini, J.D., 2006. Radar observations of Comet P/2005 JQ5 (Catalina). *Icarus* 184, 285–288.
- Jenniskens, P., and 15 colleagues, 2002. Dust trails of 8P/Tuttle and the unusual outbursts of the Ursid meteor shower. *Icarus* 159, 197–209.
- Keller, H.U., Britt, D., Buratti, B.J., Thomas, N., 2004. In situ observations of cometary nuclei. In: Festou, M.C., Keller, H.U., Weaver, H.A. (Eds.), *Comets II*. Univ. of Arizona Press, Tucson, pp. 211–222.
- Lamy, P.L., Toth, I., Jorda, L., Weaver, H.A., Groussin, O., A'Hearn, M.F., 2008. Hubble Space Telescope observations of the nucleus of Comet 8P/Tuttle. *Bull. Am. Astron. Soc.* 40, 393.
- Licandro, J., Tancredi, G., Lindgren, M., Rickman, H., Gil Hutton, R., 2000. CCD photometry of comet nuclei. I: Observations from 1990–1995. *Icarus* 147, 161–179.
- Mann, R.K., Jewitt, D., Lacerda, P., 2007. Fraction of contact binary Trojan asteroids. *Astron. J.* 134, 1133–1144.
- Nolan, M.C., Harmon, J.K., Howell, E.S., Campbell, D.B., Margot, J.-L., 2006a. Detection of large grains in the coma of Comet C/2001 A2 (LINEAR) from Arecibo radar observations. *Icarus* 181, 431–441.
- Nolan, M.C., Harmon, J.K., Howell, E.S., Benner, L.A., Giorgini, J.D., Ostro, S.J., Campbell, D.B., Margot, J.L., 2006b. Radar observations of Comet 73P/Schwassmann-Wachmann 3. *Bull. Am. Astron. Soc.* 38, 504.
- Noll, K.S., 2006. Solar System binaries. In: Daniela, L., Sylvio Ferraz, M., Angel, F.J. (Eds.), *Asteroids, Comets, Meteors (IAU 229)*. Cambridge Univ. Press, Cambridge, pp. 301–318.
- Noll, K.S., Levison, H.F., Grundy, W.M., Stephens, D.C., 2006. Discovery of a binary Centaur. *Icarus* 184, 611–618.
- Noll, K.S., Grundy, W.M., Chiang, E.I., Margot, J.-L., Kern, S.D., 2008. Binaries in the Kuiper belt. In: Barucci, M.A., Boehnhardt, H., Cruikshank, D.P., Morbidelli, A. (Eds.), *The Solar System beyond Neptune*. Univ. of Arizona Press, Tucson, pp. 345–363.
- Oberst, J., Giese, B., Howington-Kraus, E., Kirk, R., Soderblom, L., Buratti, B., Hicks, M., Nelson, R., Britt, D., 2004. The nucleus of Comet Borrelly: A study of morphology and surface brightness. *Icarus* 167, 70–79.
- Ostro, S.J., 1993. Planetary radar astronomy. *Rev. Mod. Phys.* 65, 1235–1279.
- Richardson, D.C., Walsh, K.J., 2006. Binary minor planets. *Annu. Rev. Earth Planet. Sci.* 34, 47–81.
- Scheeres, D.J., 2007. Rotational fission of contact binary asteroids. *Icarus* 189, 370–385.
- Sheppard, S.S., Jewitt, D.C., 2004. Extreme Kuiper Belt Object 2001 QG₂₉₈ and the fraction of contact binaries. *Astron. J.* 127, 3023–3033.
- Snodgrass, C., Lowry, S.C., Fitzsimmons, A., 2008. Optical observations of 23 distant Jupiter family comets, including 36P/Whipple at multiple phase angles. *Mon. Not. R. Astron. Soc.* 385, 737–756.
- Walsh, K.J., Richardson, D.C., Michel, P., 2008. Modeling asteroid spin-up with cohesion. *Bull. Am. Astron. Soc.* 40, 498.
- Waniak, W., Borisov, G., Drahus, M., Bonev, T., Czart, K., Küppers, M., 2009. Rotation of the nucleus, gas kinematics and emission pattern of Comet 8P/Tuttle: Preliminary results from optical imaging of the CN coma. *Earth, Moon, Planets* 105, 327–342.
- Weidenschilling, S.J., 2002. On the origin of binary transneptunian objects. *Icarus* 160, 212–215.
- Weissman, P.R., Choi, Y.J., Lowry, S.C., 2008. CCD photometry and radii of eight Jupiter-family comets. *Bull. Am. Astron. Soc.* 40, 387–388.
- Woodney, L., Schleicher, D.G., Bair, A.N., 2008. Rotational properties of Comet 8P/Tuttle. *Bull. Am. Astron. Soc.* 40, 415.